Journal of Low Temperature Physics, Vol. 60, Nos. 1/2, 1985

A Comparison of the ^{3}He Melting Curve, $T_c(P)$ Curve, and the Susceptibility of Lanthanum-Diluted Cerium Magnesium Nitrate below 50 mK

J. M. Parpia, W. P. Kirk, P. S. Kobiela, and Z. Olejniczak

Department of Physics, Texas A&M University, College Station, Texas

(Received December 28, 1984)

The ac susceptibility of lanthanum-diluted cerium magnesium nitrate has been compared to the temperature scales as derived from the (P, T) relation determined by Halperin and that was measured recently by Greywall. It is found that the susceptibility does not obey a simple Curie-Weiss law over the temperature range between 1 and 50 mK. The results of these calibrations are also used to determine the temperatures for the second-order phase transitions into the superfluid phases of ^{3}He at several pressures. These $T_c(P)$ values are compared to results of earlier experiments that used thermometry based on the susceptibility of platinum as well as other thermometry techniques.

1. INTRODUCTION

Three common "thermometers" for use in the millikelvin region are the susceptibility of platinum, the diluted electronic paramagnetic material LCMN (lanthanum-doped cerium magnesium nitrate), and the melting curve of ^{3}He. The platinum NMR thermometer, through the Korringa relation or via the Curie law susceptibility, has been used widely below 10 mK.[1-3] The accuracy of the platinum scale was established against nuclear orientation thermometry[4] and later against the NBS SRM 768 fixed points,[5] although some systematic discrepancies were noted against the latter. However, no direct comparison has been made between platinum NMR and the melting curve of ^{3}He, except very recently (J. Hook, Manchester University, personal communication). In comparisons between platinum and LCMN, two independent groups[1,2] observed highly consistent behavior between these two thermometers down to 0.3 mK. The "platinum thermometer" is the basis of a number of in-house temperature scales, most notably those of the Helsinki,[1] Cornell,[2] and Bell Labs[3] groups. By contrast,

0022-2291/85/0700-0057$04.50/0

the other major thermometric agent in use is the diluted electronic paramagnetic salt LCMN in a ratio of 4–5% cerium to lanthanum. This dilution is used with the expectation that the ordering temperature will be suppressed well below 1 mK, while maintaining a reasonable Curie constant. A comparison of the LCMN thermometer to the zero-sound attenuation in ^{3}He implied that the thermometer showed Curie–Weiss behavior between 10 and 1.5 mK. This measurement, together with others, formed the basis of the "La Jolla" temperature scale.[6]

The (P, T) relation[7,8] along the melting curve offers some advantages in relating temperature scales to one another. First, the (P, T) relation is relatively insensitive to sample purity and ambient magnetic fields. The temperature scale is truly thermodynamic in origin, being derived from the Clausius–Clapeyron equation. Lastly, the melting curve thermometer offers three "fixed points" at the A, B, and T_s (solid ordering) transitions, all occurring below 3 mK, in addition to a continuous (P, T) relation above 1.1 mK. The work described in this paper relates to a comparison of the susceptibility of LCMN to the melting curve as determined by Halperin *et al.*[7] and the recent work by Greywall.[8] In addition, we have observed the superfluid transitions at eight pressures between 0 and 29.15 bar. By comparing the temperatures of these transitions through the measured susceptibility of LCMN, an intercomparison of the temperature scales in use in other laboratories is possible.

2. EXPERIMENTAL DETAILS

The comparisons between the thermometers were carried out on a nuclear demagnetization cryostat to temperatures below 1 mK. The two thermometers used in these measurements are similar to those described elsewhere[8,9] and are mounted on a nuclear stage[10] as described below and illustrated in Fig. 1.

2.1. Melting Curve Thermometer

The melting curve thermometer's heat exchanger, consisting of 0.07-μm silver powder pressed in a copper body, had an integral 4-40 copper screw, which was threaded into the copper body of the heat exchanger. A separate fill capillary entered the melting curve cell, allowing it to be pressurized independently of the main heat exchanger. The capacitance of the strain gauge element was monitored with a GR 1615A capacitance bridge, and detected with an Ithaco 391A lock-in amplifier. The excitation voltage for the bridge had to be reduced to approximately 0.5 V p-p in order that no noticeable heating occurred.

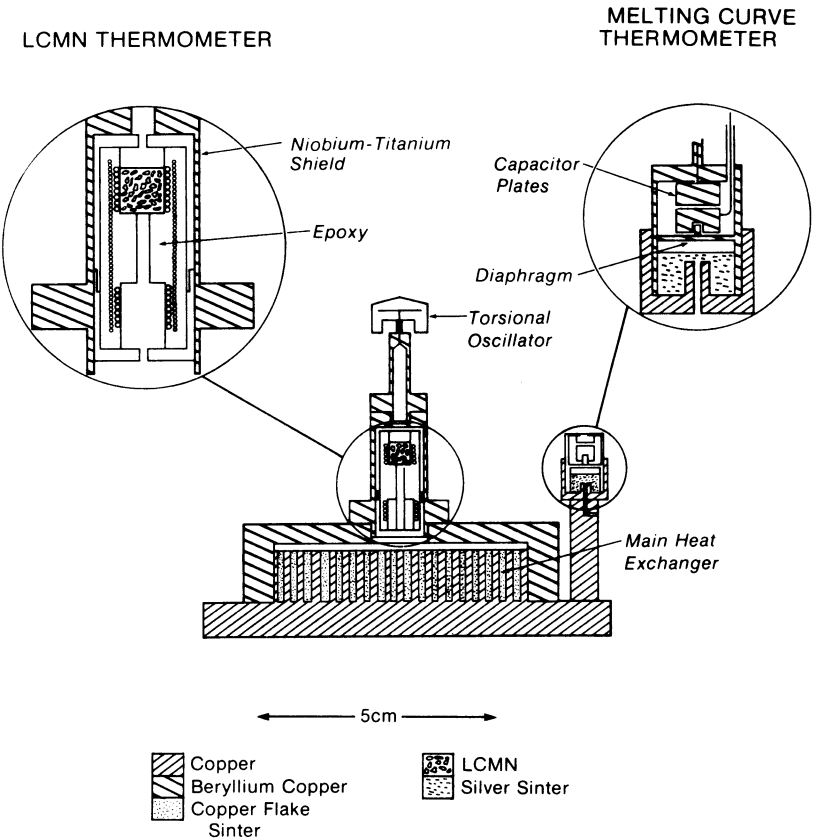

Fig. 1. A schematic of the heat exchanger for the nuclear demagnetization refrigerator. The torsional oscillator and the main ^{3}He cell heat exchanger are shown relative to the two thermometers. Enlargements of the two thermometers show the details of the construction.

The capacitor element was found to have ample sensitivity despite its small size. We found that the capacitance changed from 6.9 pF at 0 bar to 21 pF at 35 bar. The reference pressure gauge was a Paroscientific Instruments (Redmond, Washington) quartz pressure transducer, model 2900-AS-002, which was used to calibrate the melting curve thermometer. This transducer has subsequently been checked against a standard dead weight tester and found to agree with the manufacturer's calibration equation to within ±3 mbar over the entire range. The calibrations were performed at

~1.5 K, and the expression used to fit the capacitance, C, was

$$P = \sum_{n=0}^{3} A_n / C^n$$

with an accuracy of ±0.2 mbar.

Since the calibration of the strain gauge element was subject to a hydrostatic head correction of the order of 10 mbar/m of ^{3}He and since the value of this pressure head was not easily determined in our apparatus, we elected to normalize our pressures to the pressure of the minimum in the melting curve in order to resolve this problem. We found that a pressure head of 12.6 mbar was necessary to bring the calibrated pressure into agreement with the measured value of $P_{\min} = 29.316$ bar.[7] This value of the pressure head is in reasonable agreement with estimates that include the temperature gradient in the fill capillary. It should be noted that in order to verify that the measured minimum pressure was not altered by the formation of a solid layer across the sinter in the cell, the initial pressure with which the cell was filled was varied from 34 to 29.8 bar. At the beginning of any measurement sequence, the pressure at the minimum was initially found to be hysteretic at the level of 1 mbar. However, upon repeated cycling through the minimum, the observed minimum pressure was seen to drop monotonically to a value that was independent of the initial filling pressure and did not vary from other measurements, during a given experimental run, by more than ±0.5 mbar.

2.2. LCMN Thermometer

The LCMN thermometer consisted of a right circular cylinder 5 mm in diameter and 5 mm high, packed to ~50% density with 100 mg of 5% cerium-, 95% lanthanum-diluted CMN. The secondary susceptibility coils and the primary coil for the excitation were located within a cylindrical Nb-Ti shield. The shield had end caps that were drilled with four 1-mm-diameter holes to establish thermal contact. The whole assembly was immersed into the liquid sample and provided virtually hysteresis- and thermal gradient-free thermometry for a torsional pendulum device mounted directly above it.

The susceptibility coils were part of a superconducting flux transformer and were made of Nb-Ti alloy with Formvar insulation. The leads were fed through a set of solder-coated Cu-Ni and Nb tubes to shield out magnetic fields. The tubes were greased internally to prevent vibration-induced microphonic pickup of any trapped flux. The coils were connected to a SHE model HX-MFP rf SQUID. The susceptibility bridge used to null out the signal to the SQUID was a standard design, except that it incorporated a

Gertsch model RT-7 ratio transformer for additional resolution. Excitation levels of ~1 V proved to be adequate in terms of signal-to-noise ratio at no detectable self-heating.

3. CALIBRATION OF THERMOMETERS

3.1. Calibration of LCMN

In order to compare the melting curve of ^{3}He to the susceptibility of LCMN, we adopted the following procedure. The liquid ^{3}He cell was filled at 1.5 K and pumped with a charcoal dipstick to maintain the pressure at or near 0 bar. The melting curve sample was set at 34 bar to ensure that a solid-liquid mixture with a relatively high liquid-to-solid ratio would be present at low temperatures. Finally, the high temperature (~1.5 K) reading of the susceptibility of the LCMN thermometer was recorded, since this was the value used for the imbalance of the astatic pair.

We elected to carry out the calibration of the LCMN in two "segments." First, the dilution refrigerator was used to cool the nuclear stage without energizing the main demagnetization solenoid. The lowest temperature attained was ~5.9 mK. The heat switch was left on and the readings of the melting curve thermometer and the LCMN susceptibility were allowed to equilibrate, typically over 3-4 h. Measurements of the capacitance and the susceptibility were recorded and a heat load applied to the mixing chamber of the dilution refrigerator. The temperature was allowed to equilibrate and the measurements repeated. This procedure was carried out to a temperature of 45 mK, at which point the magnet was energized for a demagnetization.

A demagnetization of the nuclear refrigerator was carried out to below 1 mK. The capacitance of the melting curve thermometer's strain gauge at the A, B, and T_s features was noted in the subsequent warmup. The indicated pressure P_A was found to be $34.345_5 \pm 0.003$ bar, relative to the value of 29.316 ± 0.003 bar at the minimum. Our P_A value is different from that found by Halperin (34.342 bar).[7] The P_A value on subsequent demagnetizations was found to agree with 34.345_5 within ± 0.0005 bar. The pressures were then referenced to our value of P_A, that is, all calibrations were derived from the published (P, T) relations, where it is understood that the pressures are referred to the value at the A transition, P_A.

3.2. Low Temperature "Fixed Points"

The calibration was extended to include four fixed points below 3 mK, three identifiable with features along the melting curve and the fourth with the superfluid transition in the liquid at 0 bar, $T_c(0)$. The term "0 bar" refers

to a nominal pressure, the actual pressure on the cell possibly being as high as 10 mbar due to the pressure head of ^{3}He in the fill capillary.

The criterion for the selection of the calibration points is that they should be relatively insensitive to calibration errors in the pressure while being reproducible in temperature, and therefore transferable among laboratories. The temperatures assigned to the A transition follow from measurements of the liquid entropy at melting pressure and also from the high temperature expansion of the solid entropy's departure from the spin-$\frac{1}{2}$ disordered state. Greywall[8] has recently adopted a hybrid approach of using the values of the slope of the melting curve dP/dT as determined from Halperin *et al.*,[7] but incorporating the low temperature superconducting fixed point of tungsten* as the scaling point for the temperature scale. He arrived at a temperature of 2.708 mK for the A transition, and consequently all the temperatures of the low temperature fixed points on this scale are decreased by ~1.8%. Small additional differences in the two scales above 20 mK are also noted.

The A feature is an intrinsically nonhysteretic transition, which, due to the sharp increase in the specific heat of the liquid, results in a perceptible change in the rate of change of pressure dP/dT at a constant rate of cooling or heating dT/dt. When the pressure was plotted against the LCMN susceptibility, we observed a kink in the trace. It should be emphasized that should the thermal contact between the liquid ^{3}He and the nuclear stage be improved, or if the rate of change of temperature were to be decreased, the magnitude of the kink would diminish. In fact, in the course of the experiment a certain amount of hysteresis was observed at T_A. This was probably instrumental in origin. The results on traversing the A transition in both directions are plotted in Fig. 2a. It is evident that the hysteresis in the LCMN reading was smaller than that measured by our melting curve thermometer. The hysteresis in the value assigned to χ_A is on the order of 1 μK, while the corresponding effect in pressure is 0.1 mbar or ~3.3 μK.

The B transition, being first order, exhibits a large amount of hysteresis. However, it has been observed that the transition displays little or no superheating and provides an exceptionally clean signature associated with the latent heat (see Fig. 2b). In Fig. 2b we plot the pressure trace against the output of the LCMN bridge. The rate of change of pressure is essentially zero while the liquid undergoes the phase change within the melting curve thermometer. Subsequently, after the B→A transition is complete, the pressure change is accelerated, while the temperature within the melting curve cell approaches that of the nuclear stage.

*NBS SRM 768 device and 15.57 mK for the transition temperature for tungsten.

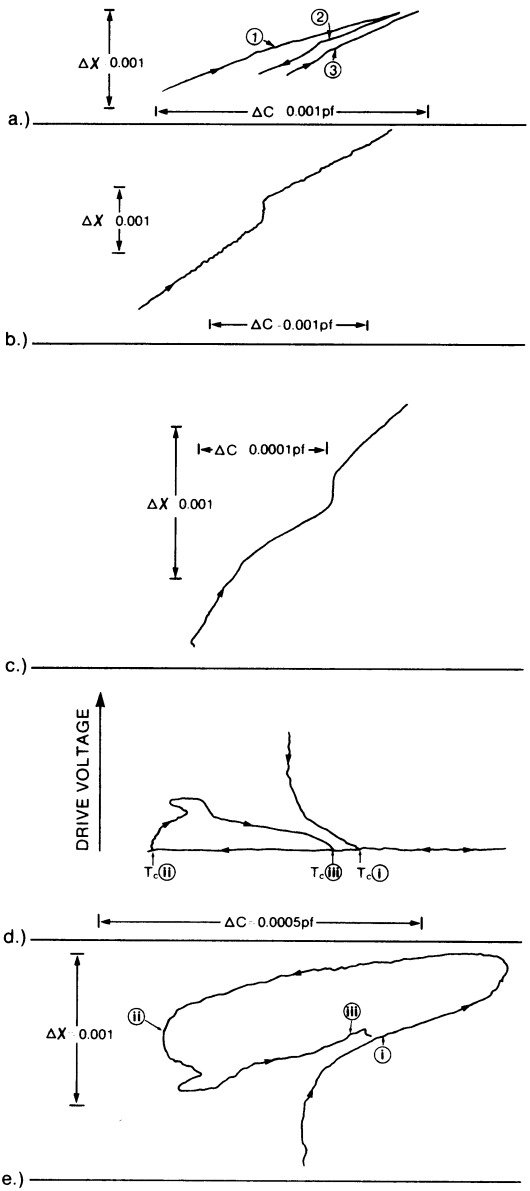

Fig. 2. The signatures of the superfluid transition for (a) the A transition, (b) the B transition, (c) the solid transition, and (d, e) the transition in the liquid cell. The horizontal axis is the output of the melting curve thermometer; in parts a–c and e, the vertical scale is the output of the LCMN thermometer, while in d the vertical scale is the dissipation of the torsion oscillator cell, signaling the onset of superfluidity. For a discussion of the hysteresis, see the text. In the trace of the A transition, ① and ③ refer to traces taken while warming, while ② was taken on cooling. In parts d and e, (i) and (iii) refer to traces taken while warming and (ii) to the signature on cooling.

The final significant feature along the melting curve is the ordering transition in the solid. This transition is thought to be first order,[3] with an ~40% change in the entropy associated with it. The solid transition displayed a large degree of hysteresis both while warming and cooling and was therefore a difficult feature to establish with accuracy. On cooling, the typical trace displayed little or no evidence of a latent heat in our device; instead, the rate of change of pressure appeared to decrease by a factor of three at moderate rates of cooling (10^{-7} K/sec). Our observation was that this slope change usually occurred at a pressure ~0.3 mbar higher than the true ordering transition. On occasions when the transition was traversed rapidly, a small backstep was seen after the appearance of the slope change. Similar effects were seen on warming; however, on one run, we were able to control the temperature sufficiently well so as to reduce the warming rate to 0.3 nK/sec and we found that a noticeable latent heat could be discerned. This effect is shown in Fig. 2c, where we plot the output of the melting curve thermometer against the LCMN bridge output. The latent heat is visible as the "step" feature. It should also be noted that Greywall saw no hysteresis at this resolution in his cell, and it may be reasonable to conclude that geometrical effects are significant.

The final fixed point is one associated with the low pressure or "0-bar" transition to the B phase of the superfluid. This point was selected since it provides another pressure-independent fixed point in the liquid cell. It was found that the liquid transition occurs at an LCMN susceptibility 0.7% lower than that for the solid transition. In Fig. 2d, we have plotted the dissipation in our torsional oscillator cell against the capacitance of the melting curve thermometer, and in Fig. 2e we have simultaneously plotted the LCMN susceptibility against the capacitance. It is evident that no feature can be clearly identified with the transition in Fig. 2e. By transferring the pressure reading at points (i)-(iii) in Fig. 2d to their values in Fig. 2e, it can be seen that the hysteresis in the LCMN thermometer is less than 0.3 μK, while that for the melting curve thermometer is approximately 0.2 mbar or 5.5 μK. Attempts to reduce the hysteresis with the melting curve cell were unsuccessful. Additionally, we have reported erroneously[12] that the 0-bar transition occurred at 1.137 mK relative to the transition in the solid cell of 1.1 mK. This result was based on an earlier calibration, where we did not look for or attempt to reduce hysteresis. Consequently a thermal gradient of 30 μK was present during that measurement. Our present value expressed as the ratio of the temperature of the transition to the superfluid state in the liquid at 0 bar to the temperature of the solid ordering transition at melting pressure is given by $T_c(0)/T_s = 1.00_7 \pm 0.02$, with the errors arising from the hysteresis shown in Fig. 2.

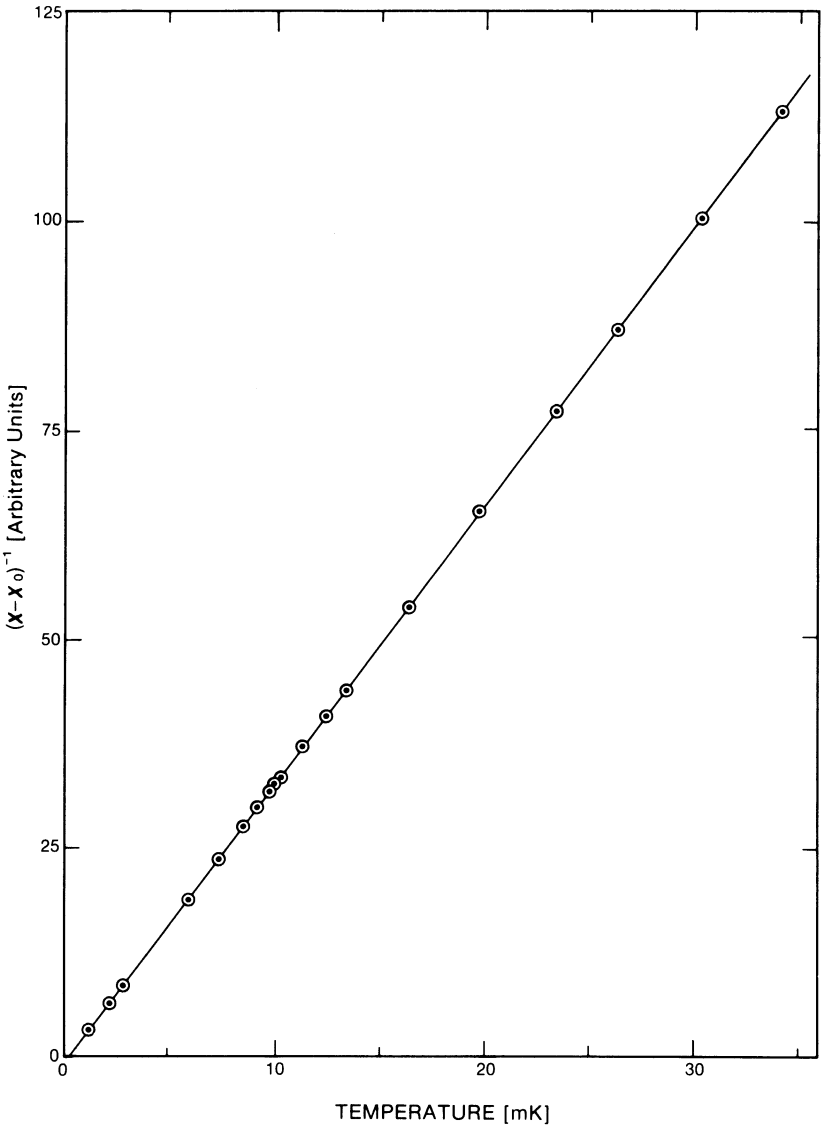

Fig. 3. The inverse susceptibility of the LCMN salt plotted against the temperature as determined from the melting curve thermometer and the pressure-temperature relation as measured by Halperin *et al.*[7] Note that the susceptibility appears to correspond to the Curie-Weiss law.

3.3. Fit Equations

The susceptibility of paramagnetic salts is commonly fit to the Curie-Weiss law by plotting the inverse susceptibility $(\chi - \chi_0)^{-1}$ against the temperature and using the resulting temperature intercept to determine the shape correction factor Δ, which is related to the Weiss temperature. We have plotted our data in this form in Fig. 3 to illustrate the inherent limitations of this approach. In Fig. 3, we have used the temperatures derived from the work of Halperin *et al.*,[7] noting that on this scale little difference would be visible if we plotted, in addition, the temperatures as found by Greywall.[8] It is clear that the calibration points appear to agree with the Curie-Weiss law with high precision, perhaps the only exception being the very lowest temperature point. However, it is precisely the lowest temperature points that are most susceptible to deviations due to the nature of the interactions between adjacent spins. In order to expose the deviation of the susceptibility from the Curie-Weiss law it is instructive to plot

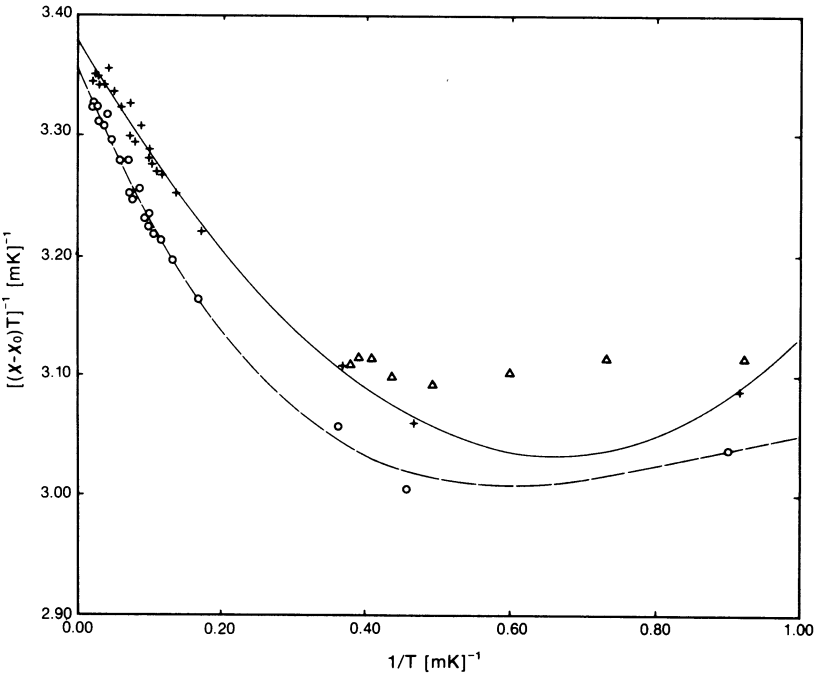

Fig. 4. The inverse of the LCMN susceptibility times the temperature plotted against the inverse of the temperature for temperatures defined by the melting curve relations of (○) Halperin *et al.*[7] and (+) Greywall.[8] (△) The values of the LCMN susceptibility at the superfluid transition, using as temperatures the results of the recent work of Greywall.[8]

$[(\chi-\chi_0)T]^{-1}$ against the inverse temperature (Fig. 4). In this plot, the differences between the Halperin and Greywall temperature scales are readily apparent as an offset in the Curie constant (the inverse of the high temperature intercept). The goodness of fit to the usual Δ shape correction term can also be examined by noting that the slope in this plot is simply the negative of the Δ term divided by the Curie constant. It can be seen that the data do not agree with a simple Curie-Weiss law as suggested by the linear fit of Fig. 3. We chose to fit the LCMN susceptibility to the equation

$$[(\chi-\chi_0)T]^{-1} = A_0 + A_1/T + A_2/T^2 + A_3/T^3$$

and found that the third-order fit was justified in the case of the Halperin melting curve scale. We have not treated χ_0, the high temperature bridge-balance point, as an adjustable parameter. If the value of χ_0 is adjusted, it is possible to fit the LCMN susceptibility to a Curie-Weiss law over a limited range of temperatures. This also has the effect of depressing the

TABLE I

The Measured Susceptibilities of the Calibration Points, Together with the Temperatures Assigned to These Points Using the Published (P, T) Relations of Halperin[7] and Greywall[8]

χ(LCMN),[a] arbitrary units	T_{Halperin}, mK	T_{Greywall}, mK
0.011494	44.831	44.550
0.0122945	40.014	39.729
0.013589	34.172	33.891
0.0147252	30.371	30.095
0.016298	26.252	25.985
0.017727	23.283	23.024
0.020131	19.763	19.524
0.023450	16.335	16.116
0.026949	13.757	13.561
0.027675	13.432	13.242
0.029400	12.510	12.328
0.031670	11.421	11.244
0.034600	10.380	10.219
0.0357035	9.998	9.837
0.0363375	9.827	9.673
0.038568	9.197	9.049
0.0411458	8.556	8.414
0.047177	7.379	7.253
0.058369	5.897	5.795
0.123603	2.752	2.708
0.157590	2.177	2.138
0.302070	1.108	1.089

[a] Note that the high temperature ($\approx$1.5 K) bridge-balance point reading (χ_0) of 0.004784 has not been subtracted from the values of the susceptibility.

TABLE II

The Fit Parameters for the Third-Order Fits to the Equation

$$[(\chi - \chi_0)T]^{-1} = \sum_{n=0}^{3} (A_n / T^n)$$

Coefficient	Halperin[7]	Greywall[8]
A_0	3.362	3.381
A_1	−1.454	−1.016
A_2	1.904	0.701
A_3	−0.768	0.065

value of Δ. We would like to emphasize that such a procedure is not justified and should therefore be avoided. Our data points for the two temperature scales are plotted in Fig. 4 along with the third-order fits. We also list the calibration points in Table I and the fit parameters in Table II.

4. COMPARISON TO OTHER TEMPERATURE SCALES

The "phase diagram," or more correctly, the second-order phase transition line between the normal fluid and the superfluid phases of ^{3}He from P_A, T_A at the melting pressure to P_0, T_0 at 0 bar, represents, in principle, a transferable temperature standard similar to the vapor pressure curve for ordinary gases. In order to compare our calibrations to those of other workers we have measured the temperatures of the superfluid transition at eight pressures. However, we would like to emphasize that such a comparison is valid only in the limited region between 1 and 3 mK.

TABLE III

The Measured Susceptibility at the Superfluid Transition at Eight Pressures, Together with the Values of the Transition Temperature as Assigned from Fits of the Susceptibility (this work) to the Melting Curve Equations of Halperin[7] ($T_{Halperin}$) and Greywall[8] ($T_{Greywall}$)

P, bar	χ(LCMN), arbitrary units	$T_{Halperin}$,[7] mK	$T_{Greywall}$,[8] mK	$(T_c(P)_{Greywall})^a$ mK
0.00	0.30207	1.1082	1.0891	1.080
2.18	0.24028	1.4089	1.3986	1.362
5.10	0.198550	1.7153	1.6985	1.6634
10.0	0.16460	1.0740	2.0456	2.0232
15.4	0.14574	2.3430	2.3056	2.2888
19.96	0.13628	2.5052	2.4628	2.4410
24.47	0.13034	2.6190	2.5731	2.5567
29.15	0.12644	2.6994	2.6511	2.6434

[a]The temperatures assigned to these transitions are from the $T_c(P)$ equations of Greywall.[8]

In order to facilitate the comparison, the values of the LCMN susceptibility at which superfluid transitions at a particular pressure were recorded are listed in Table III. These values of the susceptibility were obtained by following a procedure similar to that outlined in the description of the determination of the liquid transition at 0 bar, with the difference being that the torsional oscillator's dissipation was plotted directly against the LCMN bridge output. By utilizing our calibration equations, the corresponding temperatures for the superfluid transition were determined and are presented along with those calculated from the recent work of Greywall[8] in Table III.

Since the only closed form equation for the $T_c(P)$ relation in the literature is given in the recent work of Greywall,[8] we have chosen to display the data in the form of differences from this equation rather than attempt to display all of the phase diagrams on one plot. In Fig. 5 we have plotted $T_c(P) - T_c(P)_{\text{Greywall}}$ against the transition temperatures at the corresponding pressures from the closed form expression. It is evident that over this region of temperature, the temperature scales differ from one another by $\sim 160\ \mu$K at most.

However, in the course of measurements on the superfluid phases of ^{3}He and possibly on other systems at low temperatures, the relevant parameter is the reduced temperature (i.e., the temperature normalized to the transition temperature). In order to allow a simple comparison with other scales, we have calculated the ratio of the temperature at the A transition at melting pressure to that of the 0-bar superfluid transition. The results are shown in Table IV, and show a discrepancy of approximately 12%.

To effect a more direct comparison among the temperature scales, we fitted the $T_c(P)$ data of the other groups with a cubic spline fit, and used this function to interpolate between data points. We then computed the

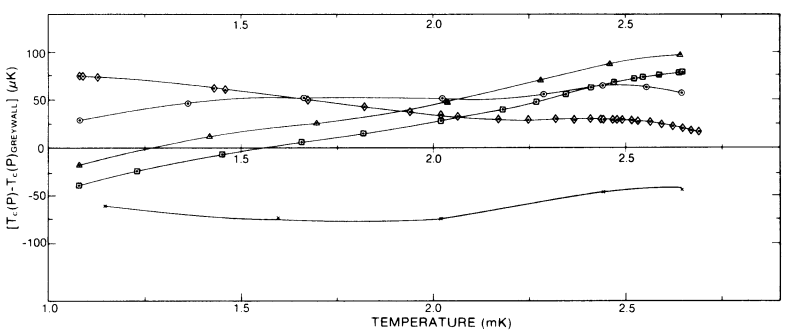

Fig. 5. The differences in the results of the (△) Cornell, (□) Helsinki, (◇) La Jolla, (×) Manchester, and (○) Texas A&M groups from the $T_c(P)$ relation of Greywall.[8]

TABLE IV

The Ratio of the Temperature of the A Transition at Melting Pressure to the Temperature of the Superfluid Transition at 0 bar

	This work	Cornell[2]	Manchester[a]	La Jolla[6]	Greywall[8]	Helsinki[1]
$T_A/T_c(0)$	2.48	2.62	2.61	2.36	2.51	2.68

[a] J. Hook, personal communication.

transition temperatures for our measured pressure values. The resulting set of T_c points were fit to our Halperin-based melting curve scale with a linear fit. However, it is expected that this function will only provide an approximate means of comparison between temperature scales, since by inspection of the differences in Fig. 5, higher order terms (or experimental inaccuracy) exist in the data making such a comparison difficult.

The linear fits to the data have been performed so as to relate the Helsinki,[1] La Jolla,[6] and recent data of Greywall[8] to our scale. The resulting equations are

$$T_{mc} = -0.080\,(\pm 0.014) + 1.0406\,(\pm 0.006)\,T_{LJ}$$

$$T_{mc} = +0.132\,(\pm 0.006) + 0.9444\,(\pm 0.003)\,T_{HS}$$

$$T_{mc} = +0.024\,(\pm 0.011) + 1.0130\,(\pm 0.005)\,T_{GR}$$

where T_{mc} is the Halperin-based melting curve scale (this work) and T_{LJ}, T_{HS}, and T_{GR} are the temperatures of the La Jolla,[6] Helsinki,[1] and Greywall[8] scales, respectively. All temperatures are in millikelvins.

In principle, due to the scaling of the temperatures in the Greywall temperature scale, the relation between our temperature scale and that of Greywall[8] should be a ratio of precisely 1.018, instead of the value 1.013 together with the small offset reported here. We cannot offer a simple explanation for this result. The rms deviations from the fitted functions are on the order of 8 μK, with evidence for a systematic higher order term.

5. CONCLUSION

It is our conclusion that the use of LCMN as a secondary thermometry device presents significant difficulties, which through the exercise of reasonable precautions can be minimized. Our comparison with the melting curve indicates that if the LCMN susceptibility is fitted over a range below 50 mK, a simple Curie-Weiss law does not fit the data to sufficient accuracy. The apparent discrepancy between this result and other measurements may be due to the use of the high temperature or bridge-imbalance term as an additional fitting parameter in the "Curie-Weiss law." Furthermore, it is

evident that the common practice of only fitting the susceptibility to the $T_c(P)$ line (between 1 and 3 mK) can easily result in erroneous extrapolations to higher and lower temperatures and should be avoided unless a direct comparison can be made to data over a range of up to 20 mK.

Another difficulty encountered with the use of melting curve thermometers is the small but significant discrepancy in the measured values of the pressure at the A transition. Calibrations utilizing the melting curve should therefore be performed using the measured values of $P - P_A$ rather than using a value of P_A inferred from the measured value of P_{min}. By doing so, the calibration would presumably also minimize errors in attempting to measure with millibar accuracy over a 5-bar pressure interval.

In this work we have carefully avoided making judgments as to the accuracy of the various temperature scales. It is clear that there are significant differences in the scales and that each technique has its adherents. It should be noted that a complete set of measurements over a wide range of temperatures against the melting curve thermometer permits the conversion of one scale to another through the melting curve pressure–temperature relation. For this reason alone, the adoption of the melting curve as an interim standard for comparison can be useful.

Within the constraints that we have noted, we would conclude that LCMN thermometry continues to serve as a high-resolution secondary thermometer in the millikelvin regime. However, it is also clear that the interactions between the electronic spins are more complex than previously assumed. Consequently, it is mandatory to calibrate the thermometer over as wide a range of temperatures as feasible, and that the calibration have special emphasis on the low temperature region, while avoiding the use of the high temperature susceptibility as a fitting parameter.

ACKNOWLEDGMENTS

The authors would like to thank Dr. John Hook of Manchester for allowing them to use the recent Manchester $T_c(P)$ results. We would also like to acknowledge conversations with Dr. Dennis Greywall. This research was supported in part by the NSF through grants DMR-8218279 and DMR-8205902. One of us (J. M. P.) is the recipient of an Alfred P. Sloan Research Fellowship.

REFERENCES

1. T. A. Alvesalo, T. Haavasoja, M. T. Manninen, and A. T. Soine, *Phys. Rev. Lett.* **44**, 1076 (1980); and T. Haavasoja, Thesis, Helsinki University of Technology (1980).
2. E. K. Zeise, Thesis, Cornell University (1981), unpublished.
3. D. D. Osheroff and C. Yu, *Phys. Lett.* A 77, 458 (1980).

4. P. M. Berglund, H. K. Collan, G. J. Ehnholm, R. G. Gylling, and O. V. Lounasmaa, *J. Low Temp. Phys.* **6**, 357 (1972).
5. E. Lhota, M. T. Manninen, J. P. Pekola, A. T. Soine, and R. J. Soulen, Jr., *Phys. Rev. Lett.* **47**, 590 (1981).
6. D. N. Paulson, M. Krusius, J. C. Wheatley, R. S. Safrata, M. Koláč, T. Těthal, K. Svec, and J. Matas, *J. Low Temp. Phys.* **34**, 63 (1979).
7. W. P. Halperin, F. B. Rasmussen, C. N. Archie, and R. C. Richardson, *J. Low Temp. Phys.* **31**, 617 (1978).
8. D. S. Greywall, *Phys. Rev.* **B31**, 2675 (1985).
9. D. S. Greywall and P. A. Busch, *J. Low Temp. Phys.* **46**, 451 (1982).
10. J. M. Parpia, W. P. Kirk, P. S. Kobiela, T. L. Rhodes, Z. Olejniczak, and G. N. Parker, *Rev. Sci. Instr.*, **56**, 437 (1985).
11. O. Avenel, M. Bernier, D. Bloyet, P. Piejus, E. Varoquaux, and C. Vibet, in *Proceedings of the 14th International Low Temperature Physics Conference*, M. Krusius and M. Vuorio, eds. (North-Holland, Amsterdam, 1975), Vol. 4, p. 64.
12. P. S. Kobiela, Z. Olejniczak, W. P. Kirk, and J. M. Parpia, in *Proceedings of 17th International Conference on Low Temperature Physics*, U. Eckern, A. Schmid, W. Weber, and H. Wühl, eds. (North-Holland, Amsterdam, 1984), Part II, p. 1173.